Energy 333 (2025) 137542

Contents lists available at ScienceDirect

Energy

journal homepage: www.elsevier.com/locate/energy

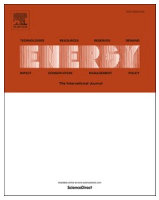

4E analysis of an integrated system using nitrogen expansion refrigerant and LH_2 cold energy for a compression-free liquid air energy storage

Fatma Yehia [a,b,1], Akram Ali Nasser Mansoor Al-Haimi [a,b,1], Yuree Byun [c], Junseok Kim [c], Chuangji Feng [a,b], Yu Cao [a,b], Yesom Yun [c], Jeongwon Kim [c], Chao Yang [b,*], Lihua Liu [b,**], Jihyun Hwang [c,***]

[a] University of Science and Technology of China (USTC), Hefei, Anhui, 230026, PR China
[b] Guangzhou Institute of Energy Conversion, Chinese Academy of Sciences, Guangzhou, 510640, PR China
[c] Department of Energy Engineering, Korea Institute of Energy Technology, Naju, 58330, Republic of Korea

ARTICLE INFO

Handling editor: L Luo

Keywords:
Liquid air energy storage
Liquefied hydrogen
Nitrogen refrigeration
Exergy analysis
Economic analysis

ABSTRACT

This study introduces an integrated energy storage system combining nitrogen expansion refrigeration(N_2R) and liquefied hydrogen (LH_2) cold energy in a compression-free Liquid Air Energy Storage (LAES) system. The purpose is to enhance power generation efficiency and reduce energy losses by utilizing cold energy from hydrogen regasification and nitrogen expansion cycles. Thermodynamic analysis indicates exceptional round-trip efficiencies of up to 329.62 %, specific energy consumption (SEC) of 0.13 kWh/kg-air, and energy savings of 3590 kW (20.4 % carbon emission reduction). Exergy analysis reveals a high efficiency of 66 %, highlighting minimal thermodynamic irreversibilities. Economic analysis confirms significant viability with a Net Present Value (NPV) of $65.7 million, an Internal Rate of Return (IRR) of 29 %, and a payback period (PBP) of 2.67 years. These results establish the integrated approach as a highly efficient, sustainable, and economically attractive solution for energy storage.

1. Introduction

The increasing global demand for sustainable and efficient energy storage technologies has spurred significant advancements in LAES systems. These systems are recognized for their potential to facilitate large-scale energy storage with high efficiency while maintaining a minimal environmental impact [1]. LAES uses excess electrical energy, typically sourced from renewables or generated during off-peak times, to condense and liquefy atmospheric air at cryogenic temperatures. This liquid air (LA) is stored in insulated tanks until energy demand rises. At that point, it is expanded through a turbine to produce electricity efficiently [2]. Recent developments have underscored LAES as a promising solution to modern energy storage challenges [3]. Morgan et al. [4] provided a comprehensive analysis of LAES technology, emphasizing its potential to achieve grid-scale energy storage, achieving a round-trip efficiency (RTE) of approximately 60 %. Adedeji et al. [5] observed that optimizing ambient air conditions could enhance system performance by 11.7 %. Two investigations were conducted by Xue et al. [6] and Guizzi et al. [7] reported RTEs of about 50 % for the optimized standalone LAES system. Additionally, a study by Guo et al. [8] explored the dynamics of cold energy transfer within packed beds, while Wang et al. [9] proposed an approach using a single pressurized fluid to streamline cold energy recovery, reaching an RTE near 50 %. However, one of the major limitations of LAES is its relatively low RTE, which typically falls within the range of 50–60 % [10,11]. To improve performance and cut costs, integrating cryogenic energy storage technologies can be effective [12]. Salem and Khaira [13] highlighted that the LAES system hybridization by integrating alternative refrigeration techniques and utilizing cold energy sources could significantly enhance system efficiency. This leads to 89 % liquid yields, 32 % lower power use, and 28 % higher exergy efficiency than conventional designs. Naquash et al. [14] explored the integration of LH_2 regasification with

* Corresponding author.
** Corresponding author.
*** Corresponding author.
E-mail addresses: yangchao@ms.giec.ac.cn (C. Yang), liulh@ms.giec.ac.cn (L. Liu), jihyun.hwang@kentech.ac.kr (J. Hwang).
[1] Authors contributed equally.

https://doi.org/10.1016/j.energy.2025.137542
Received 25 April 2025; Received in revised form 21 June 2025; Accepted 11 July 2025
Available online 16 July 2025

Liquefied Natural Gas(LNG), natural gas liquids(NGL), and liquid helium production. Their approach utilized the cold energy from LH_2 to aid in the separation of NGL and helium from natural gas, then liquefying methane-rich gas. Park et al. [15] introduced an innovative cryogenic energy storage framework designed for energy retention by employing two distinct cold energy transfer techniques. This Multi-Cryogenic Energy Storage system achieved an impressive RTE of 85.1 %, surpassing the conventional bulk power management efficiency cap of 75 %. Yehia et al. [16] presented an innovative hybrid system integrating a nitrogen single-effect mixed refrigerant cycle with the liquefaction of air, coupled with regenerative Rankine cycles, achieving an RTE of 168.64 %. Further advancements by Park et al. [17] investigated a hybrid model incorporating LAES with LNG cold energy utilization. Their findings revealed an electrical RTE of 187.4 % alongside an achieved exergy efficiency of 75.1 %, demonstrating the potential of cryogenic integration to maximize system effectiveness. Expanding on LNG cold energy utilization, recent studies have explored alternative refrigeration techniques and diverse cold energy sources, including LH_2, to optimize system efficiency [18,19]. The LH_2 regasification presents an opportunity to harness its cryogenic cold energy, which can be integrated into LAES to enhance efficiency and reduce energy consumption [20]. Given the thermodynamic similarities between LH_2 and LNG regasification, this integration is thermodynamically favorable. Although LH_2 liquefaction reduces hydrogen volume for easier storage and transportation, it is a highly energy-intensive carrier compared to other hydrogen alternatives [21–23]. Efficient regasification can reclaim part of that energy, making it valuable for cryogenic energy storage applications [24,25]. Various methods, such as direct expansion [26,27] and integration with Brayton and organic Rankine cycle(ORC) [28–30], have been explored for optimizing energy recovery [31]. Incorporating LH_2 cold energy into LAES presents a promising approach to achieving higher efficiency and economic viability in large-scale energy storage. Recent studies have explored this integration, focusing on the thermodynamic and economic benefits. Yu et al. [32] investigated the recovery and application of cold energy from isolated LH_2 storage tanks within LAES systems, demonstrating the potential for improving efficiency through the use of cold energy sources. Kim et al. [18] introduced three distinct LH_2 regasification approaches integrated with LAES, achieving RTEs of 51.20 %, 126.50 %, and 150.20 % and highlighting economic benefits from repurposing LH_2 cold energy to reduce air liquefaction costs and supporting sustainable energy storage. Further improvements by Kim et al. [33] introduced a dual-stage power generation system that combines LH_2 regasification with LAES, achieving an exceptional RTE of 403.5 %. This setup used seawater and LH_2 cold energy to surpass 100 % efficiency, showcasing notable energy savings and economic potential. These studies highlight the critical role of LH_2 cold energy in optimizing energy storage systems, particularly when paired with advanced refrigeration technologies. Additionally, ORC technology has emerged as a promising solution for energy recovery, particularly in applications involving low-temperature heat sources to generate electricity [34,35]. The potential of the ORC technology for LNG/LH_2 cold energy recovery has been explored in several studies. For instance, She et al. [36] proposed an innovative hybrid LAES model that utilizes wasted heat from compression as an ORC input. while a vapor compression refrigeration cycle functions as a heat sink. This hybrid approach boosted electricity generation with an RTE gain of 9–12 % compared to standard LAES setups. Zhang et al. [37] introduced a hybrid model combining LAES and ORC systems using LNG cold energy. This configuration reached up to 70.51 % electricity storage efficiency under standard conditions, significantly better than standalone systems. Similarly, Peng et al. [38] explored using pressurized propane to recover LNG cold energy, optimizing air liquefaction, and achieving a maximum RTE of 88 %. Kim [39] proposed a novel LH_2 refueling station design integrating a direct expansion cycle and ORC. This setup showed a 38.6 % drop in energy use compared to conventional LHRS systems, confirming ORC's strength in tapping LH_2 cold energy for better efficiency and cost-effectiveness. Various ORC systems, including single-stage, parallel two-stage, and cascade two-stage configurations, have been explored to enhance the efficiency of LH_2 cold energy utilization in power generation. These studies show ORC's adaptability and effectiveness in converting low-temperature energy into power, particularly when integrated with refrigeration strategies. Despite these advancements, the integration of nitrogen expansion refrigerants with LH_2 cold energy in LAES systems remains underexplored. This represents a significant research gap, as the combined use of these technologies could further enhance system efficiency and reduce energy losses. Nitrogen expansion refrigerants are emerging as a viable alternative to traditional refrigeration techniques in cryogenic systems [40–42]. Nitrogen is an inert, non-toxic, and abundant gas, making it an ideal working fluid for refrigeration cycles [43,44]. As a working fluid in refrigeration cycles, nitrogen can undergo expansion in a turbine to produce significant cooling effects, which can be effectively utilized to reduce the energy input required for air liquefaction in LAES systems [45,46]. Chenchen et al. [47] presented an advanced LNG cold energy-coupled LAES system integrating a novel N_2R cycle to enhance cooling efficiency. Nitrogen expansion lowered temperatures, supplying high-grade cold energy to the cold box. The RTE improves from 74.42 % to 77.33 % as LNG temperature decreases from −135 °C to −145 °C, indicating increased efficiency. Under a −135 °C LNG temperature and 51.04 t/h consumption rate, the exergy efficiency reached 62.9 %. The LCOE was 0.102 USD/kWh, a 12.5–24.2 % cost cut compared to current storage options. Similarly, Zhang et al. [48] proposed an LNG cold energy-coupled LAES system incorporating an N_2R cycle. The system's RTE improved from 72.83 % to 77.33 % under similar LNG conditions. At optimal operation (−135 °C and 51.04 t/h flow), the exergy efficiency also reached 62.9 %. Its LCOE was 0.077 USD/kWh—a 34–42 % reduction—proving its economic strength. Altogether, integrating nitrogen expansion refrigerants, LH_2 cold energy, and ORC technologies presents a novel, high-efficiency pathway to overcome traditional LAES limitations. Combining LH_2's high energy density, nitrogen's cryogenic properties, and ORC's recovery efficiency offers strong potential to advance energy storage systems.

Conventional LAES systems face several key limitations, including high energy consumption due to mechanical air compression, low round-trip efficiency (typically below 70 %), and minimal utilization of available cryogenic energy from hydrogen infrastructure. Additionally, their reliance on compression equipment increases system complexity and operational cost. These limitations reduce their attractiveness for integration into future decarbonized energy systems. The proposed approach addresses these issues through a compression-free design that harnesses the cold exergy of LH_2 and nitrogen expansion, thereby enhancing both thermodynamic and economic performance.

To bridge existing research gaps, this study aims to introduce a novel integration of a nitrogen expansion refrigerant and LH_2 cold energy within a compression-free LAES system. The primary focus is on enhancing power generation efficiency and reducing energy losses. A comprehensive 4Es: energy, exergy, economic, and efficiency analyses will be conducted to assess the system's thermodynamic performance, economic feasibility, and overall operational efficiency. The research focuses on optimizing power utilization, improving energy recovery, and maximizing resource efficiency. A comparative analysis with alternative refrigeration techniques will be performed to quantify potential advantages, including enhanced energy recovery and improved system performance. This research aspires to contribute innovative insights into the design of a sustainable and high-performance energy storage system by leveraging multi-source energy integration. This study introduces a novel approach in which air compression is entirely eliminated by integrating the cold energy from LH_2 regasification and nitrogen expansion refrigeration. Unlike conventional LAES systems that rely on energy-intensive air compression, the proposed system utilizes the cryogenic potential of LH_2 and the cooling capacity of an N_2R cycle to achieve direct air liquefaction, thereby significantly enhancing energy efficiency and reducing parasitic losses. This system aligns with

global energy transition goals by eliminating fossil-based compression and supporting scalable, hydrogen-integrated, low-emission energy storage infrastructure.

2. Process concept, design description, and assumptions

2.1. Process concept

The proposed integrated LH_2-N_2R-LAES system utilizes the cold energy from LH_2 and N_2R to enhance the efficiency of LAES without relying on conventional compression methods. In this compression-free design, the system bypasses mechanical air compression by using a cascade of heat exchangers and cryogenic cold energy sources—specifically, LH_2 and N_2R cycles—to cool the air to liquefaction temperatures. This method not only reduces energy consumption but also improves thermodynamic performance by minimizing irreversibilities. Fig. 1 illustrates the schematic of the proposed system. In the design, the key innovation is the integration of N_2 expansion with the utilization of LH_2 cold energy, effectively replacing the traditional compression steps required for air liquefaction. Initially, LH_2, stored as a liquid, is regasified to produce hydrogen gas (GH_2), which can be used for various end-user applications. In conventional systems, regasification requires thermal energy from external sources, but in this design, the cold energy generated during LH_2 regasification is repurposed for the liquefaction of air, eliminating the required high-energy compression stage. The process involves heating LH_2 in a series of heat exchangers (HXs), transferring the cold energy to the air, cooling it down, and facilitating its liquefaction. ORCs are also employed to generate power from the thermal gradient. Additionally, the N_2R cycle is integrated into the final stage of air liquefaction to further boost efficiency. The residual cold energy from LH_2 is used to drive a series of expanders to generate electricity, which is fed into the electrical grid. The LA is stored in cryogenic storage tanks, where it can be expanded to generate extra power as needed. Overall, this integrated system offers a highly efficient and sustainable solution by optimizing stored cold energy for dual-function energy storage and flexible energy supply.

2.2. Process design description

Fig. 2 illustrates the schematic flow of the proposed LH_2-N_2R-LAES system, which integrates an N_2R expansion cycle with the LAES system and the LH_2 Regasification process to enhance the system efficiency. The proposed system consists of three key sections: the storage section of the LAES, the direct expansion of the GH_2 section, and the release section of the LAES, in addition to two ORCs for energy recovery.

In the storage section, the LH_2 at −254.5 °C and 1.013 bar is first pressurized to 150 bars (Stream LH1) using the LH_2 Pump (P-1). The latent cold energy of the LH_2 is transferred to both air and ORCs through a series of five heat exchanger systems (HX-1-HX-5), where the LH_2 is heated during the heat transfer. As a result, the temperature of the hydrogen in a stream of LH6 increases to −55 °C. To address potential soil freezing and enhance operational safety, an additional seawater heater (H-7) is implemented to further elevate the hydrogen temperature above −55 °C. The system also incorporates two ORCs positioned between HXs to maximize energy recovery from the cold energy of hydrogen. The temperature-entropy (T-S) diagram of these ORCs is presented in Fig. 3.

The proposed system liquefies the air utilizing only the cooling potential of the LH_2, directly exchanging heat through HX-1, HX-3, and HX-5. Under ambient conditions, air must be cooled to approximately −193 °C for liquefaction, eliminating the need for additional air compression stages. −193 °C. This approach significantly enhances the RTE [18]. Prior to liquefaction, air is purified to remove impurities that may freeze during the process. The purified air enters the system at 25 °C with a flow rate of 10.30 kg/s, gradually cooling through heat exchanging with LH_2 in a three-stage HX system.

The air is cooled to −88.9 °C in HX-1 and further to −157.0 °C in HX-3. To further improve process efficiency, the system integrates an N_2R expansion cycle for additional cooling. The N_2R cycle operates with a one-stage compressor (K-1) using nitrogen as the working fluid due to its low boiling point and suitability for cryogenic applications [49]. The thermodynamic properties of the N_2R cycle are illustrated in Fig. 4, showing both T-S and pressure-enthalpy (P-H) diagrams.

The N_2R cycle starts at atmospheric pressure (1.013 bar) and 20.0 °C (stream N1) and is pressurized to 2.9 bar. The nitrogen cycle streams (N1 to N4) contribute to cooling by releasing cold energy to HX-5, where the pressure is reduced to 1.013 bar using the expander (T-1). This additional cooling lowers the air temperature to −193.8 °C, contributing to the cold energy of LH_2, allowing it to liquefy. Finally, the liquefied air is stored in an LA tank at 1.013 bar. The N_2 stream undergoes isobaric

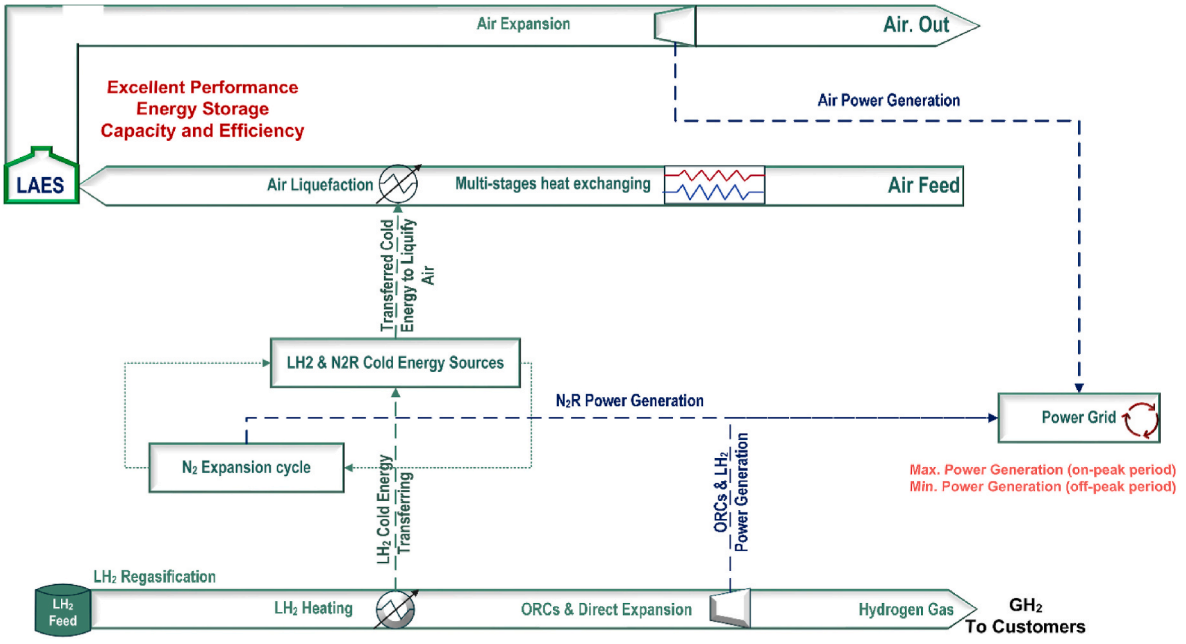

Fig. 1. The basic diagram of the LH_2-N_2R-LAES system.

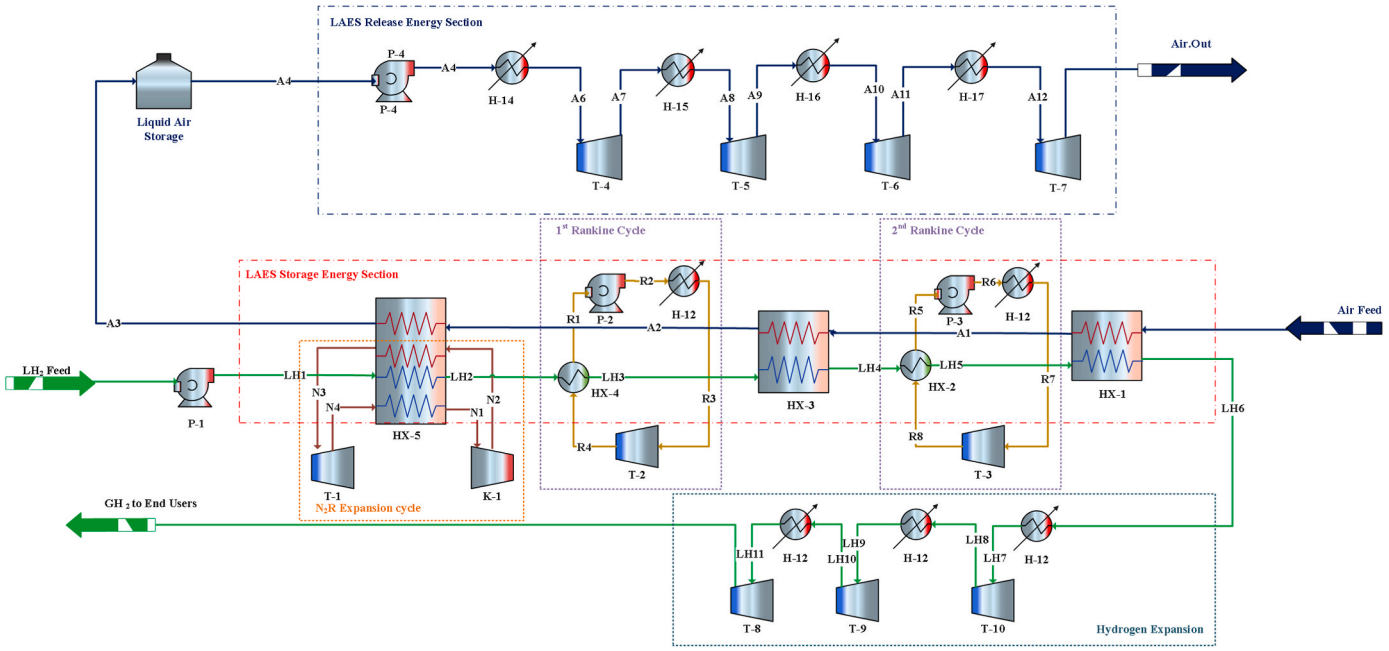

Fig. 2. The projected LH_2-N_2R-LAES system schematic diagram, including the LAES storage, LAES release, and GH_2 direct expansion sections.

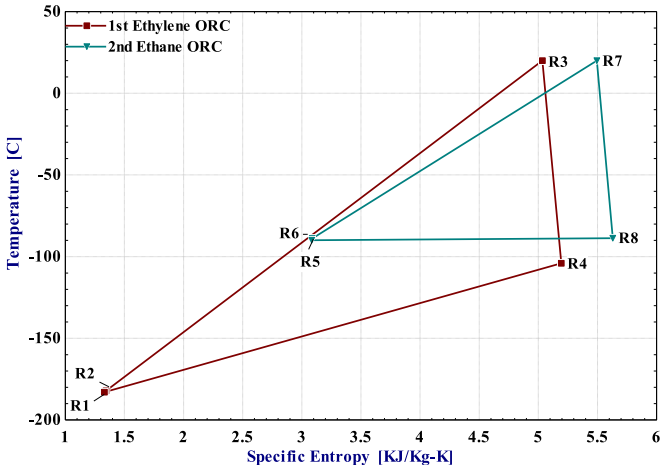

Fig. 3. The T-S thermodynamic Diagram of ORCs.

heating in HX-5 from cryogenic conditions (N4) to ambient conditions (N1), with the entire cycle simulated under single-phase assumptions. No condensation or two-phase compression occurs in the modeled N_2R cycle.

In the ORCs section, ethylene and ethane are selected as working fluids for the first and second ORCs, respectively, due to their favorable thermodynamic properties, low environmental impact, and excellent cryogenic performance [50–52]. To effectively utilize the broad temperature gradient available from LH_2 regasification, two Organic Rankine Cycles (ORCs) were implemented using ethylene and ethane as working fluids. Ethylene was selected for the ultra-low temperature zone (−185 °C to −159.7 °C) and ethane for the moderately cold range (−140 °C to −91.1 °C), based on their favorable boiling points and thermophysical properties. Ethylene condensation occurs at approximately −104.1 °C under atmospheric pressure (1.013 bar), followed by subcooling to −183.0 °C before pumping. This avoids the need for sub-atmospheric operation while enabling efficient cold energy extraction. The dual-ORC configuration improves thermal matching and reduces exergy losses compared to a single-cycle alternative, supporting higher overall system efficiency despite slightly increased capital cost. The working fluid in the first ORC is liquefied in HX-4 via heat exchange with LH_2, increasing hydrogen temperature from −185.1 °C to −159.7 °C. A pump (P-2) increases the working fluid pressure from 1.013 bar to 35 bar, after which it is vaporized to 20 °C using seawater (H-1). The vaporized working fluid then expands through an expander (T-2), reducing pressure from 35 bar to 1.013 bar and generating shaft work. In the second ORC, the working fluid (ethane) is liquefied in HX-2 by exchanging heat with LH_2, heating hydrogen from −140 °C to −91.14 °C. A pump (P-3) pressurizes the working fluid from 1.013 bar to 22.0 bar, and it is subsequently vaporized to 20 °C via seawater heating (H-2). Afterward, the high-pressure vapor undergoes expansion through an expander (T-3), reducing pressure from 22 bar to 1.013 bar, producing shaft work. The thermodynamic properties of Rankine and N_2R cycle working fluids are summarized in Table S1.

The pressurized hydrogen undergoes sequential expansion to produce shaft work. Initially, the high-pressure hydrogen is heated in two seawater heaters (H-8 & H-9) before expanding in three-stage expanders (T-8 to T-10). This sequential expansion reduces hydrogen pressure from 150 bar to 104, 70, and finally 45 bar. Since the typical pipeline for hydrogen transportation generally operates within a pressure range of 34.5–82.7 bar [18,53], the system assumes a final distribution pressure of 45 bar to align with industry standards. Finally, the release section operates in parallel with the direct expansion of GH_2. The LA from the liquid storage tank is pressurized to 230.0 bar using a pump (P-4). Following pressurization, the LA undergoes a sequential heating and expansion process through seawater heaters (H-3 to H-6) and four air turbines (T-4 to T-7), generating electricity. The T-S diagrams for air charging and discharging processes are presented in Fig. 5.

2.3. Process assumptions

For assessing the proposed LH_2-N_2R-LAES performance, Aspen HYSYS V14.0 software was used for the design and simulation of the system. The Peng-Robinson equation of state (EoS) was employed to compute the thermodynamic properties of LAES, N_2R, and ORCs, respectively [54,55]. At room temperature, GH_2 consists of approximately 75 % ortho-hydrogen (ortho-H_2), where the nuclear spins are aligned in the same direction, and 25 % para-hydrogen (para-H_2), where

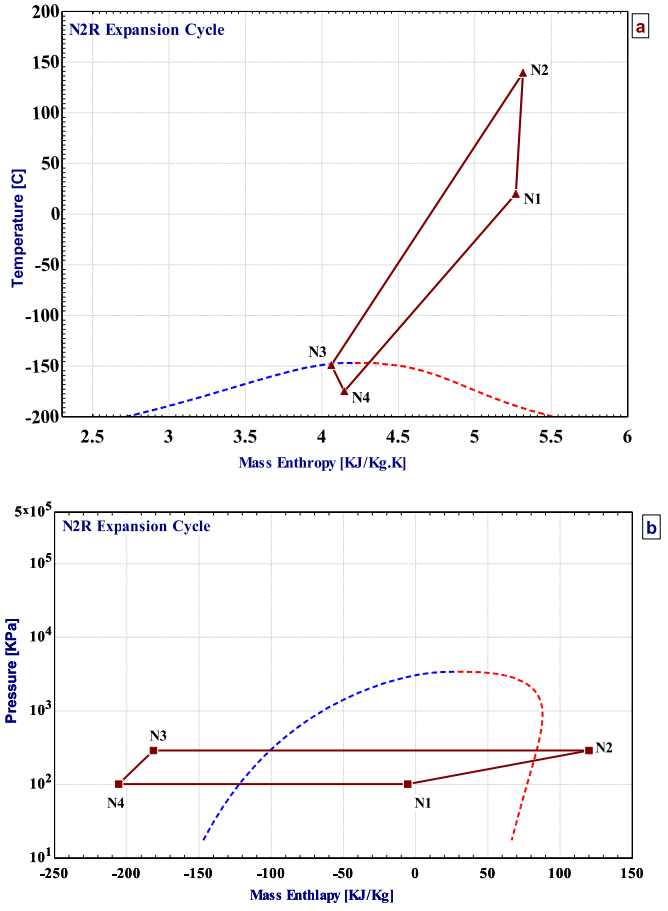

Fig. 4. Thermodynamic diagrams of the N_2R expansion cycle: (a) Temperature–Entropy (T–S) diagram, and (b) Pressure–Enthalpy (P–H) diagram. All nitrogen streams in the N_2R cycle are simulated under single-phase conditions. Apparent intersections with the saturation dome are visual artifacts due to plotting resolution and do not represent two-phase behavior. The heat exchange from N4 to N1 in HX-5 is modeled as an isobaric process at approximately 1.013 bar.

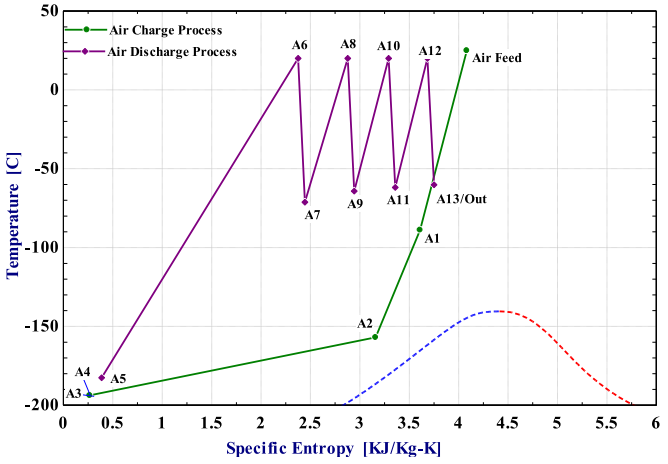

Fig. 5. The air charging and discharging thermodynamic T-S diagram.

the nuclear spins are oriented in opposite directions [56,57]. In contrast, the LH_2 predominantly exists as para-H_2, which is in a lower energy state compared to ortho-H_2 [30,58]. To accurately represent the properties of hydrogen in this context, the modified Benedict-Webb-Rubin EoS is utilized [59,60]. It should be noted that the conversion between ortho-H_2 and para-H_2 is not considered in the proposed process. The following assumptions were made for the simulation of the LH_2-N_2R-LAES process.

- The simulation is performed under steady-state conditions, with on-peak operation assumed to be 10 h/day.
- The global convergence tolerance was set to 1×10^{-4}, and tear streams were automatically adjusted by the solver to ensure closure of mass and energy balances.
- The heaters outlet temperature is set at 20 °C; the minimum temperature difference (MTD) across all heat-exchangers was maintained at 3 °C with no pressure drop consideration.
- Shell-tube heat exchangers were configured in a counter-current flow mode.
- The N_2R compression ratio is set to 2.86, not exceeding 3.5, and the expansion ratio is set to less than 1 [61].
- Heat losses between the system's unit operations and the surroundings are neglected, and the boil-off rate is considered negligible at 0.05 vol%/day [62].
- LH_2 product is transported to end users at a pressure of 45 bar [53]. For evaluating power generation and consumption by expanders, compressors, and pumps, isentropic efficiency is applied according to the specifications in Table S2. The composition and operating conditions of the LH_2-N_2R-LAES process feed, as well as the working fluids for the ORCs and N_2R, are detailed **in** Table 1.

3. Performance assessment methods

A thorough performance assessment of the proposed system is carried out using four key thermodynamic procedures that are frequently utilized in energy systems analysis [63]. These procedures include heat exchange assessment, energy assessment, which encompasses RTE, SEC, coefficient of N_2R performance (COP) calculations based on the first law of thermodynamics, and exergy assessment aligned with the second law of thermodynamics. To achieve an in-depth understanding of system functionality, the process includes three primary sections: the storage section of the LAES, the direct expansion of the GH_2 section, and the release section of the LAES, supplemented by two additional ORCs. This configuration is designed to optimize the utilization of cold energy and maximize electricity generation. The heat exchange assessment focuses on the recovery of LH_2 cold energy, forming the basis for further evaluations of system efficiency. Following this, the energy assessment is performed to quantify heat flow and determine overall energy efficiency. The assessment further incorporates RTE calculations, offering critical insights into the effectiveness of energy storage within the

Table 1
Basic Assumptions and Specifications of the proposed LH_2-N_2R-LAES process.

Items	Values
LH_2 feed conditions	
Inlet temperature	−254.50°C
Pressure	1.013 bar
Mass flow	2.0 kg/s
Air feed conditions	
Inlet temperature	25°C
Pressure	1.013 bar
Mass flow	10.30 kg/s
N_2R Expansion Conditions	
Temperature	20.0 °C
Pressure	1.013 bar
Mass flow	0.2200 kg/s
1st ORC Composition	
- Ethane	1.0000
2nd ORC Composition	
- Ethylene	1.0000

integrated system. Exergy indicators are applied to further examine system feasibility to determine available work potential and validate the thermodynamic efficiency of the LH_2-N_2R-LAES process. Beyond thermodynamic assessments, an economic assessment is performed by applying the Net Present Value (NPV) methodology to assess the financial viability of the projected system, ensuring a comprehensive assessment of both performance and cost-effectiveness.

3.1. Heat exchanging assessment

A detailed heat exchange analysis was performed to investigate the interactions between hot and cold streams in MSHEs. Composite curves were formulated, integrating both temperature and heat transfer (THCC) to explore the temperature fluctuations alongside the dynamics of heat transfer. In the same sequence, Temperature difference composite curves (TDCC) were employed to elucidate the correlation between temperature gradients and approach temperature, providing insights into heat exchange feasibility and heat recovery potential. The MTD was adopted as a key indicator to evaluate HX performance, with a target MTD of ≤ 3 °C, ensuring sufficient temperature difference for effective heat transfer.

3.2. Energy assessment

A systematic energy assessment is performed to evaluate the efficiency and capacity of the proposed system based on the first law of thermodynamics. The assessment of system performance focuses on two primary metrics: energy efficiency and storage capability. In the evaluation of large-scale energy storage and conversion applications, the RTE is recognized as a key indicator for assessing both performance and economic feasibility [64,65]. It measures the proportion of energy recovered from the system during the utilization of stored or converted energy relative to the initial input of energy. The RTE is mathematically expressed as:

$$\eta_{RTE} = \frac{P_{net,out}}{P_{net,in}} = \frac{\varpi_{En,R} * T_{on-peak}}{\varpi_{En,S} * T_{on-\&off-peak}} \quad (1)$$

Or, using system-specific notations:

$$\varpi_{En,R} = \left(W_{ORC1} + W_{ORC2} + W_{N2R} + \sum_{i=4}^{7} W_{T,i} + \sum_{i=8}^{10} W_{T,i} \right) \quad (2)$$

$$\varpi_{En,S} = \sum_{i=1}^{4} W_{p,i} + W_{k,N2R} + Q_{LH2} - Q_{N2R} \quad (3)$$

Where η_{RTE} represents the RTE, while $P_{net,out}$, $P_{net,in}$ donate the total power outputs and net power inputs. $\varpi_{En,R}$, and $\varpi_{En,S}$ correspond to the energy released and stored in the system. W_{ORC2} , $W_{N2R,}$ and $W_{T,i}$, represent the power generated by the first and second ORCs, N_2R Cycle, and expansion systems, respectively. In contrast, $W_{p,i}$ $W_{k,N2R}$ indicate the power consumed by pumps and compressors. The cold energy supplied by liquid hydrogen and the nitrogen expansion cycle is represented by Q_{LH2} and Q_{N2R}, respectively. System power generation and consumption calculations are based on the data in Table S3. The power-release time $(T_{on-peak})$ is set at 10 h, while the storage period follows two scenarios: one involving partial storage during off-peak hours, and another considering full storage over the combined on- and off-peak period.

To further analyze liquefaction efficiency, the SEC is assessed as a critical performance metric. It provides insights into the energy required to liquefy a given mass of gas, serving as a key determinant of overall system efficiency. Enhancing the energy efficiency of liquefaction not only reduces operational costs but also minimizes environmental impacts. The SEC is mathematically represented as [18]:

$$SEC = \frac{TEC}{m_{l-air}} \quad (4)$$

Furthermore, to assess the efficiency of the nitrogen expansion cycle, the COP is used to evaluate the nitrogen expansion cycle's efficiency and its integration with the LH_2-LAES system. The proposed LH_2-N_2R-LAES configuration reflects the relationship between the useful cooling effect produced by the cryogenic working fluid and the total energy input required for the proposed process. The COP is determined using the following equation:

$$COP_{N2R} = \frac{m_{N_2} \times (h_{N_2,in} - h_{N_2,out})}{W_{total}} \quad (5)$$

Where m_{N_2} is the mass flow rate of the N_2R working fluid, $h_{N_2,in}$, and $h_{N_2,out}$ donate the enthalpies of the inlet and outlet streams, respectively, and W_{total} represents total work input.

3.3. Exergy assessment

Exergy analysis serves as a key metric for quantifying energy losses and determining the useful work potential within the proposed system [66,67]. The exergy rate is defined as:

$$EXE = m \times [(h_i - h_0) - T_0 \times (S_i - S_0)] \quad (6)$$

Where EXE represents the exergy rate, h denotes enthalpy, T is temperature, and S corresponds to entropy in the system's streams. The subscripts i and 0 refer to the thermal conditions of the equipment and ambient atmospheric conditions, respectively. The exergy balance equation is expressed as:

$$EXE_{net\_in} = \sum EXE_{in} + \sum W_{in} \quad (7)$$

$$EXE_{net\_out} = \sum EXE_{out} + \sum W_{out} = EXE_{net\_in} - EXE_{net\_destruction} \quad (8)$$

The defined variables are as follows: EXE_{net_in}, EXE_{in}, W_{in}, denote net exergy input, total exergy supplied to the system, and input work, whereas, EXE_{net_out}, and EXE_{out}, correspond to the net exergy output and total exergy output, respectively. W_{out} signifies the work generated while $EXE_{net-destruction}$ quantifies the total exergy destruction or losses across all system components. The exergy efficiency is determined using the following expression:

$$\eta_{EXE} = EXE_{net.out} / EXE_{net-in} = \left(\sum EXE_{out} + \sum W_{out} \right) \Big/ \left(\sum EXE_{in} + \sum W_{in} \right) \quad (9)$$

Therefore, to accurately assess exergy efficiency, it is essential to calculate the net exergy input, output, and destruction separately. The exergy efficiency is then determined using the following equation:

$$EXE_{net\_in} = EXE_{LH2\_in} + EXE_{Air\_in} + W_K + W_P \quad (10)$$

$$EXE_{net\_out} = EXE_{GH_2\_out} + EXE_{air\_out} + W_T \quad (11)$$

$$EXE_{net\_destruction} = EXE_{net\_in} - EXE_{net_{out}} = EXE_P + EXE_K + EXE_T + EXE_H + EXE_{HX} + EXE_{NG_{out}} + EXE_{air_{\_out}} \quad (12)$$

In this analysis, EXE_{LH2_in} represents the LH_2 stream input exergy, EXE_{Air_in} corresponds to the air stream input exergy. Similarly, the exergy losses associated with different system components are defined as follows: $EXE_P, EXE_K, EXE_T, EXE_H, EXE_{HX}$ represents the exergy losses in Pumps, Compressors, Expenders, Heaters, and heat exchangers, respectively., $EXE_{GH2\_out}, EXE_{air_{\_out}}$ denote the output exergies of GH_2, and air outlet streams. Furthermore, the exergy losses associated with each unit in the proposed process, along with their corresponding exergy

efficiency, are determined using the equations outlined in Table S4.

3.4. Economic assessment

The financial viability of the projected LH_2-N_2R-LAES system is assessed by applying the NPV method. It serves as a key metric for determining economic feasibility. The NPV is calculated using the following equation [16,68]:

$$NPV = -C_{TCI} + \sum_{\omega=1}^{n} \frac{(S_T - C_{oc} - C_{Dep})*(1-\varphi) + C_{Dep}}{(1+\tau)^n} \quad (13)$$

Where the net present value was represented by NPV, C_{TCI} denotes the total capital investment, ω denotes operating years, n refers to the plant's life, τ is the discount rate, S_T represents annual sales revenue, C_{oc} corresponds to annual operating costs, C_{Dep} denotes depreciation costs and φ is the tax rate. The capital investment estimation follows the Bare Module (BM) Cost ($C_{BM,i}$) approach, which is calculated using the purchased cost function $\left(C^0_{p,i}\right)$, following the methodology outlined by Turton et al. [69]. The cost constraints are derived using the equations listed in Table S5 [69]. In this model, K_1 , K_2, and K_3 are constant parameters. Meanwhile, "A" represents the capacity factor, which varies depending on the system equipment. For cryogenic heat exchangers, the "A" is defined as the area of heat transfer derived from the overall coefficient of heat transfer (UA), with a value obtained directly from the process simulator. The assumed heat transfer coefficient (U) is 3600 W/m^2K [70]. The capacity factors for the heaters and shell and tube heat exchangers are extracted from the Aspen Energy Analyzer, as provided in Table S6.

The annual sales revenue is calculated based on generated electricity during energy release phases, covering both on-peak and off-peak periods, as hydrogen sales are not considered in this study. The annual operational cost includes utility expenses and maintenance costs. Additionally, the annualized capital cost is determined using the capital recovery factor (CRF). The economic assumptions and cost evaluation equations are detailed in Table 2.

4. Results and discussion

The proposed LH_2-N_2R-LAES system is assessed through a thermodynamic evaluation and compared against recently reported configurations. This comparative study seeks to critically examine process performance and identify potential improvements in efficiency. Heat exchange processes are analyzed using composite curves in conjunction with exergy flow diagrams. Detailed operational parameters of the LH_2-N_2R-LAES system, including temperature, pressure, mass flow rate, enthalpy, entropy, and exergy, are summarized in Table S7.

4.1. Heat exchange assessment

Composite curves are essential analytical tools for evaluating heat transfer efficiency and optimization [76]. In many instances, the MTD between the hot and cold streams at the inlet or outlet defines the MTD when phase transitions do not occur within the heat exchanger. However, when phase changes are involved, it is crucial to assess the feasibility of maintaining effective heat exchange while avoiding temperature crossover [77]. The location of the pinch point is not restricted to the inlet or outlet; rather, it can develop within the internal structure of the HX due to phase transition effects. The proposed system incorporates an air-free compression approach to enhance heat exchange efficiency and optimize energy utilization. The absence of direct air compression reduces parasitic energy losses associated with compressing non-condensable gases, enabling more efficient cryogenic heat transfer. The system relies on a cascade of HX-1, HX-3, and HX-5 to progressively cool the air streams, leading to enhanced thermal integration. Fig. 6 represents The THCC and TDCC curves, which provide quantitative insights into the HXs performance. HX-1 serves as the initial cooling stage of air liquefication process, as depicted in Fig. 6a. A total of 1153.6 KJ/Kg_{LH2} of LH_2 cold energy is transferred to the air feed, lowering its temperature to −88.90 °C (stream A1), with MTD of 2.52 °C and the Log Mean Temperature Difference (LMTD) of 23.0 °C indicate effective heat exchange with a well-maintained temperature gradient. Subsequently, HX-3 further reduces the temperature of the air stream to −157.0 °C (Stream A2), as demonstrated in Fig. 6b. This is achieved by employing 682.8 KJ/Kg_{LH2} of LH_2 cold energy. The TDCC curve reveals an MTD of 2.46 °C and an LMTD of 16.7 °C, demonstrating minimal thermal resistance and optimized heat transfer. In the final stage, HX-5 completes the liquefaction process of air, as presented in Fig. 6c.

In this stage, the N_2R expansion cycle plays a dual role, significantly enhancing cooling capacity while recovering a 66.34 KJ/Kg_{LH2} of LH_2 cold energy to shift the work and generate power through T-1 expansion work recovery. The total cold energy transfer at HX-5 amounts to 2404.8 kJ/kg_{LH2} from LH_2, supplemented by 44.13 kJ/kg_{LN2} cold energy from the N_2R cycle. As a result, the air reaches its final liquefied temperature of −193.8 °C (Stream A3). The MTD of 3.12 °C and an LMTD of 13.9 °C highlight precise thermal management in cryogenic conditions, ensuring minimal exergy destruction and maximized heat exchange efficiency.

Fig. 7 illustrates the overall thermal exchange process in the air liquefaction and the LAES storage section of the proposed system. The system integrates multiple ORCs, facilitating enhanced heat recovery and efficiency. The heat exchange between the LH_2 stream and the ORC cycles' working fluids within the heat exchangers (HX-4 and HX-2) converts 922.20 KJ/KgLH2 and 1621.0 KJ/Kg_{LH2} of the cold energy into mechanical work for power generation. Selecting optimal low-temperature working fluids is crucial for maximizing cold energy recovery from the liquefaction process. The extent of heat exchange is directly influenced by the boiling points of these fluids, as latent heat absorption plays a critical role in cooling performance. The composite curves for hot and cold streams illustrate distinct phase transformation gaps, particularly during ethylene and ethane transitions. To meet MTD design requirements and optimize heat transfer efficiency, it is imperative to fine-tune refrigerant compositions and operational parameters, ultimately reducing exergy destruction and improving the sustainability of the LH_2-N_2R-LAES system for cryogenic energy storage and power regeneration. In the first ORC, ethylene undergoes phase change during the heating process; however, due to its narrow boiling range at 35 bars, the low flow rate, and the minimum temperature difference constraint applied in the simulation, the latent heat absorption appears as a sloped segment rather than a distinct constant-temperature plateau.

Table 2
The economic assessment assumptions.

Item	Value
Plant-life time (years)	25 [71]
Discount rate %	7 [72]
Tax rate %	25 [73]
Depreciation method	Straight line
Maintenance cost %	2 [71]
Labor cost%	0.03
Daily average of electricity price ($/kWh)	0.22 [74]
25 % daily average higher ($/kWh)	0.275
50 % daily average higher ($/kWh)	0.33
Heating utility cost	1.9×10^{-6} [75]
Electricity cost ($/kWh)	0.06 [69]

4.2. Energy assessment

An energy analysis was conducted to evaluate the performance of the proposed LH_2-N_2R-LAES system. The RTE—a standard metric for energy storage systems—was used to measure the relationship between electrical input and output. Using the formulas defined in the previous section, the calculated RTE for the off-peak storage mode reached

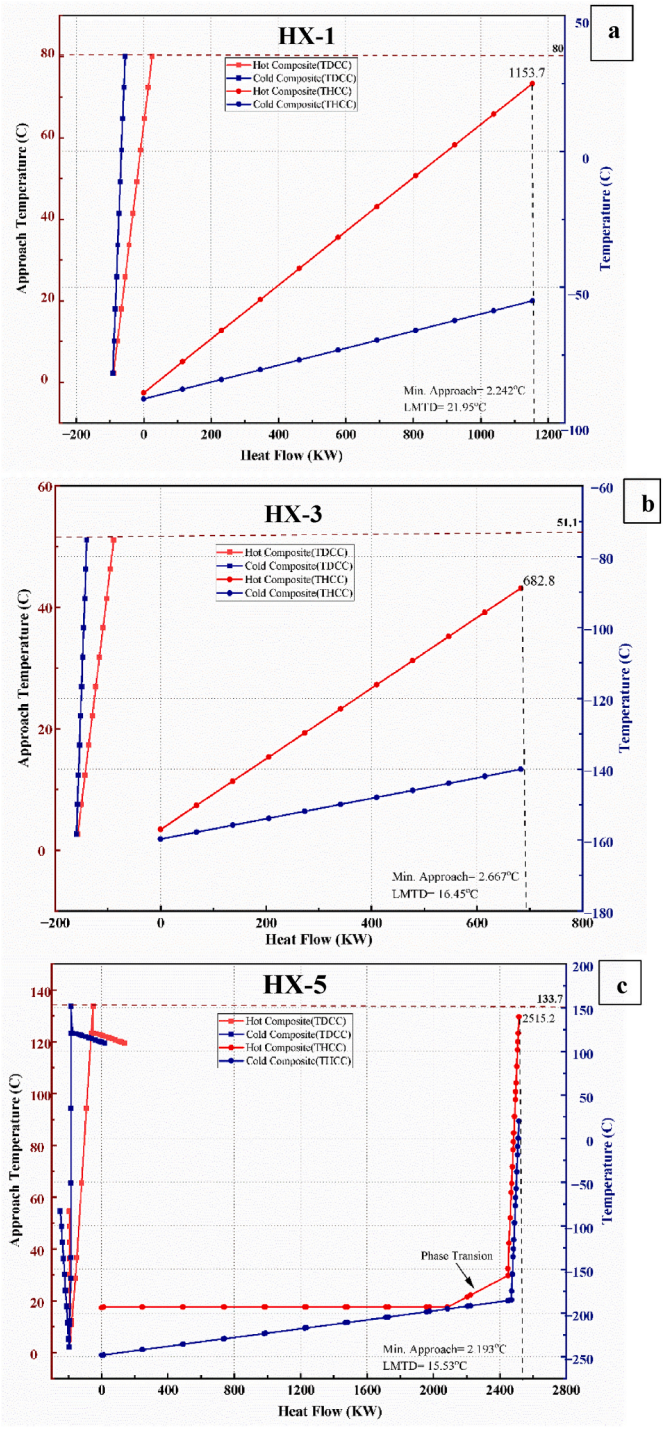

Fig. 6. The THCC and TDCC Curves of the air liquefaction process:(a)HX-1, (b) HX-3, and (c)HX-5.

192.28 %, while the highest performance was observed during the combined off- and on-peak storage scenario, achieving an RTE of 329.62 %. These findings imply that prolonged storage operation enhances the energy efficiency of the system. Typical RTE values for conventional bulk power storage systems rarely exceed 75 % [63]. However, the RTE in our integrated energy storage and LH_2 regasification process exceeds this conventional benchmark. This is primarily due to the effective utilization of cold energy recovered from LH_2, which contributes to improved system efficiency. As previously reported, RTE values exceeding 100 % are achievable when external cold energy, such as LH_2, is incorporated into the process [18,78]. Table 3 summarizes the energy contributions of the key components in the proposed system, revealing that the turbines generated a total of 7260.98 kW, whereas the compressors and pumps collectively consumed 1023.17 kW. Furthermore, the Aspen Energy Analyzer was utilized to quantify the energy benefits, demonstrating a net energy saving of 3590 kW, representing a 20.4 % saving. This corresponds to a carbon emission reduction of 0.36 kg/s, equivalent to a 20.4 % decrease, as illustrated in Fig. S1 and Table S8.

In terms of liquefaction performance, the SEC is a critical metric, reflecting the energy needed to produce 1 kg of liquefied air. The proposed air-free compression integration system achieves an SEC of 0.13 kWh/kg, showing only a 1.4 % increase compared to the optimized Cases 2 and 3 in Kim et al. [18], which also eliminates air compression stages. The slight increase is attributed to the additional work required for nitrogen compression in the N_2R cycle. Nevertheless, this SEC represents a significant reduction compared to the 0.69 kWh/kg reported for conventional LAES systems [19], again primarily due to the effective use of LH_2 cold energy [79]. Using the designated equation, the COP for the N_2R expansion cycle was calculated to be 1.98. This value surpasses the COP of 1.59 for the SMR cycle when nitrogen is used as the working fluid in LNG-LAES configurations [16]. These results suggest that the N_2R cycle provides a more effective cooling effect while also maximizing energy utilization, thereby offering enhanced overall efficiency. As such, the integration of the N_2R cycle with LH_2-LAES appears to be a promising strategy for energy-efficient applications in cryogenic power systems.

4.3. Exergy assessment

Employing equations 7–12 and presented in Table S4, the proposed system achieves a total exergy efficiency of 66.0 %, representing an improvement of approximately 15.8 % and 10.6 % compared to recent systems, such as LH-LAES-WOC and LH-LAES-WORC, which eliminate the air compression stages and exhibit exergy efficiencies of 57.0 % and 59.7 %, respectively [18]. The integration of the N_2R cycle significantly enhances the system's exergy efficiency by reducing irreversibilities and associated losses. A detailed analysis of exergy flow and associated losses within the proposed system is provided in the subsequent subsection.

4.3.1. Exergy flow

Fig. 8 depicts a systematic diagram of the exergy flow for the proposed LH_2-N_2R -LAES integrated process, illustrating exergy outputs calculated in the preceding sections. During the LAES stage, the LH2 Feed enters with an exergy content of 15653.3 kJ/kg$_{LH2}$. A significant exergy loss of 633.06 kJ/kg$_{LH2}$ occurs primarily during pressurization using the LH_2 pump. The pressurized LH_2 stream provides cold exergy totaling 6920.9.3 kJ/kg$_{LH2}$, used alongside ambient air inlet exergy of approximately −0.021 kJ/kg-air at atmospheric conditions. Of this cold exergy, 771.6 kJ/kg$_{LH2}$ is transferred to liquefy air in the initial and intermediate stages of the liquefaction process, resulting in a final air exergy of 96.6 kJ/kg-air. Additionally, two ORCs—using ethylene (first cycle) and ethane (second cycle)—are incorporated between the air liquefaction using the heat exchangers (HX-4 and HX-2) to recover waste energy and generate shaft work. The LH_2 cold exergy utilized in these cycles totals 1649.8 kJ/kg$_{LH2}$, distributed as 912.1 kJ/kg$_{LH2}$ and 737.7 kJ/kg$_{LH2}$ for the ethylene and ethane cycles, respectively.

Concurrently, the nitrogen refrigerant expansion cycle contributes cold exergy of 134.0 kJ/kg$_{N2}$, utilized to assist air liquefaction and cool the hot stream within the N_2R cycle. Additionally, N_2R exergy amounting to 49.5 kJ/kg$_{N2}$ is converted to useful work. Ultimately, the LA exergy of 721.4 kJ/kg$_{air}$ is stored in the LAES system.

In the subsequent GH_2 direct expansion stage, the exergy losses amounting to 247.1 kJ/kg$_{LH2}$ occur due to heat transfer through multi-stage seawater heaters. Simultaneously, GH_2 exergy totaling 1484.3 kJ/kg$_{LH2}$ is expanded across multi-stage expanders to produce shaft work.

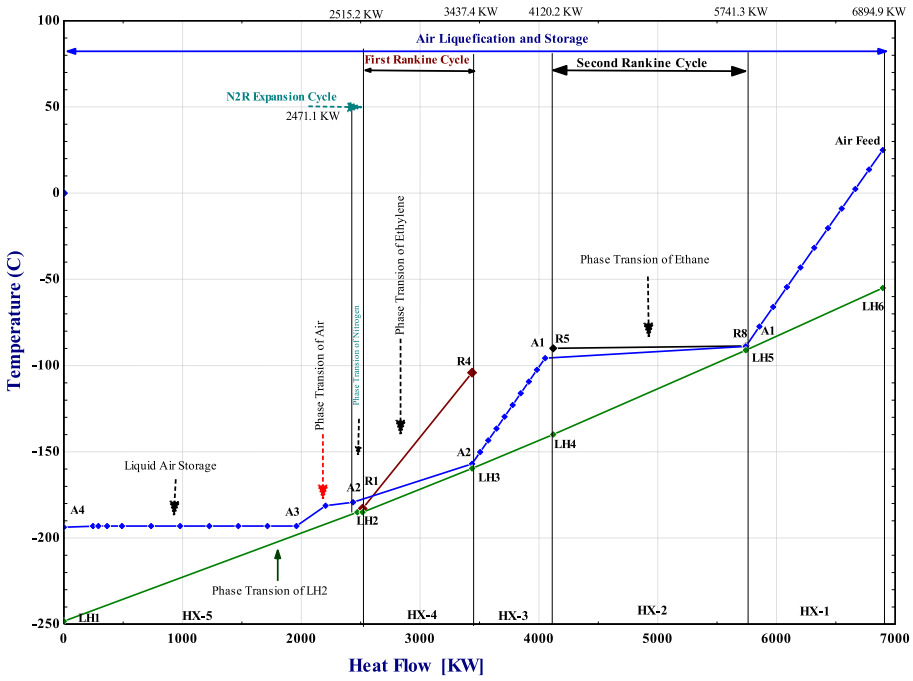

Fig. 7. The overall heat flow schematic diagram of the LAES Storage section.

Table 3
Energy consumption and generation across unit operation components (KW).

Unit	Energy consumption	Unit	Energy generation	Energy Efficiency	
P-1	563.94	T-1	573.12	RTE (Off-Peak) storage	192.28 %
P-2	10.92	T-2	278.90	RTE (Off&On-Peak) storage	329.62 %
P-3	18.32	T-3	6.25	SEC of air liquefaction	0.13
P-4	397.51	T-4	925.05	N_2R COP	1.98
K-1	32.47	T-5	917.39		
Total	**1023.17**	T-6	949.18		
		T-7	947.92		
		T-8	797.46		
		T-9	950.72		
		T-10	915.00		
		Total	**7260.98**		

Eventually, a GH_2 stream with an exergy of 4718.2 kJ/kg$_{\text{-LH2}}$ is discharged.

During the exergy release phase, the previously stored LA exergy (721.4 KJ/Kg$_{\text{-air}}$) is partially consumed, 2.9 kJ/kg$_{\text{-air}}$ for pressurization by the LA pump. Further exergy losses of (314.7 KJ/Kg-air) occur. During heat transfer to seawater heaters. Subsequently, exergy released through multi-stage expanders totals 388.9 kJ/Kg$_{\text{-air}}$, leaving a residual exergy of 14.9 kJ/kg-air discharged to the environment.

4.3.2. *Exergy destruction*

Fig. 9 illustrates the absolute exergy losses associated with each unit operation, providing detailed insights into irreversibility sources within the LH_2–N_2R–LAES integrated system. The analysis indicates that the heat exchangers and heaters represent the most significant contributors, accounting for approximately 47.91 % and 28.46 % of total exergy losses, respectively. Specifically, substantial losses occur in heat exchangers HX-5 and HX-4—approximately 5876.8 kW and 963.4 kW—predominantly due to irreversibilities associated with phase changes in the final stage of air liquefaction and considerable temperature gradients during heat exchange between the LH_2 stream and air. Additionally, the seawater heater (H-3) contributes significantly to exergy losses at the air discharge end, owing to entropy generation from large temperature differences. Pumps collectively account for 12.95 % (2125.2 kW) of total losses, followed by expanders at 10.66 % (1750.2 kW), indicating non-isentropic behaviors and heat transfer inefficiencies. Conversely, compressors have a negligible impact, contributing merely 0.02 % of the total exergy loss.

For a deeper assessment, the global and local exergy analyses were evaluated, summarizing each unit operation's exergy efficiency and loss, which is presented in Fig. 10 and S2, and Table S9. From a global perspective, the majority of units demonstrate high thermodynamic efficiency, contributing minimally to overall losses. However, unit operations such as HX-5, H-3, and P-1 dominate exergy destruction, accounting for 35.8 %, 16.2 %, and 10.6 % of system-level losses, respectively. The primary source of exergy destruction in these units lies in irreversible thermodynamic processes associated with extreme cryogenic and high-pressure conditions, which lead to significant entropy generation and degradation of useful energy. Moreover, the local exergy analysis (Fig. S2) shows that most unit operations maintain efficiencies above 95 %, reflecting optimized operation with minimal irreversibilities. However, significant exergy losses are observed in Heaters (H1–H3), where efficiencies fall below 70 %, and HX5 with an efficiency of 81.1 %, highlighting the significant scope for enhancement of the second-law efficiency of the LH_2–N_2R–LAES system by prioritizing improvements in thermal integration and exchanger effectiveness.

4.4. *Economic assessment*

The economic analysis provided a comprehensive overview of the financial performance of the proposed system. The overall economic assessment results are summarized in Table 4 and Fig. 11. The Net Present Value, a crucial economic indicator, stands at 65.7 million USD, indicating robust financial viability and potential for substantial profitability over the project's lifespan. Additionally, Table S10 provides a detailed financial breakdown of individual system components, indicating that expanders account for the highest purchase cost at approximately 8.32 million USD, followed by heaters at 1.15 million USD, heat exchangers at 0.30 million USD, pumps at 0.17 million USD, and

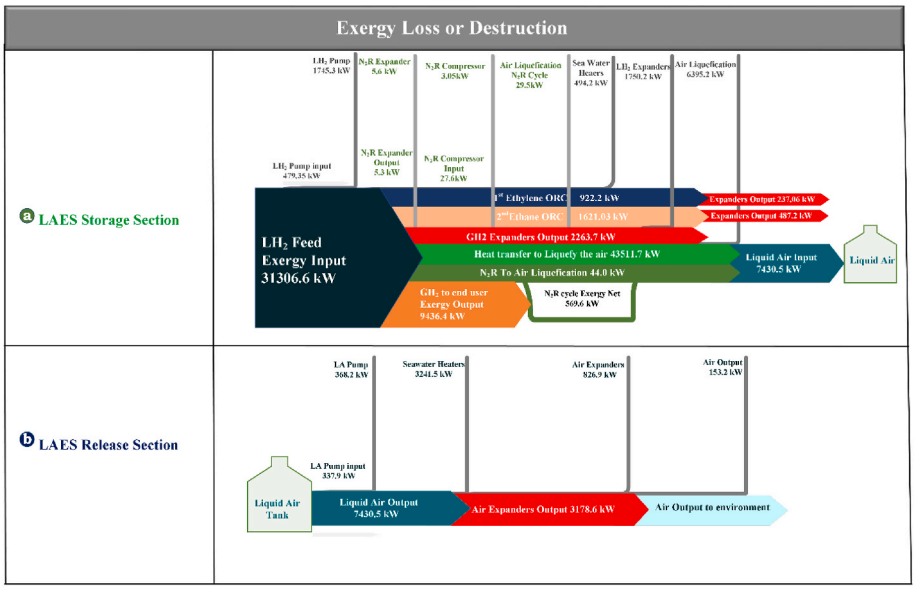

Fig. 8. The LH_2-N_2R-LAES system exergy flow, which represents the following: (a) LAES Storage and (b) LAES Release Sections.

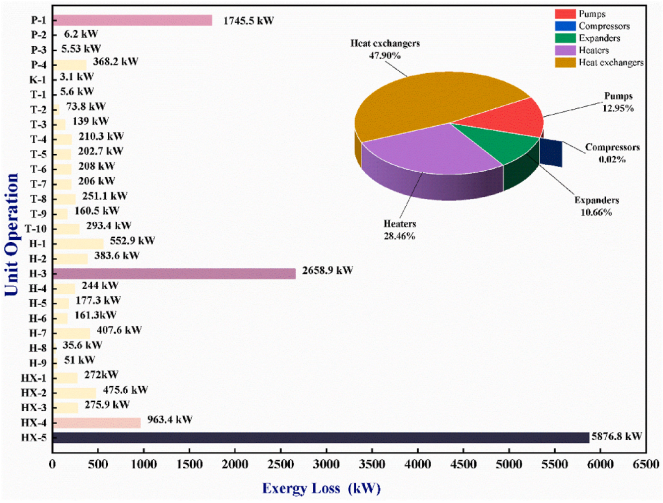

Fig. 9. The exergy loss/destruction of each unit operation associated with the projected LH_2-N_2R-LAES system.

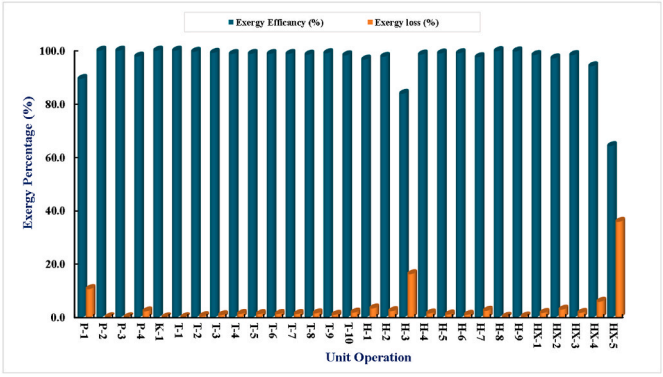

Fig. 10. The Global exergy efficiency and loss (%) of each unit operation of the proposed system.

Table 4
The overall economic evaluation of the proposed LH_2-N_2R-LAES system results.

Items	Unit	Value
Total capital cost	m$	43.34
Compressors	m$	0.07
Expanders	m$	37.31
Pumps	m$	1.64
LNG exchangers	m$	0.92
Heat exchangers	m$	0.43
Heaters	m$	2.98
Annual operating cost	m$	2.65
Electricity consumption cost	m$	0.19
Heating cost	m$	0.58
Maintenance cost	m$	1.14
Labor cost	m$	0.17
other costs	m$	0.57
Annual revenues	m$	11.89
Annualized cost	m$	6.36
IRR	%	29 %
PBP	years	2.67
Net present value		
Daily average	m$	65.69
Daily 25 % higher	m$	91.68
Daily 50 % higher	m$	117.67

compressors at 0.02 million USD.

This positive NPV results predominantly from high total revenues of electricity, amounting to approximately 297.36 million USD, which substantially surpasses the combined total capital and operating costs, as shown in Fig. 11a (Fig. 11b and c). shows the breakdown of expenditures, where the total capital cost and total operating cost are evaluated at 43.27 million USD and 66.13 million USD, respectively.

Annualized costs further delineate the economic structure, with annual capital investments constituting approximately 58.4 % and annual operation costs representing about 41.6 % of total annualized expenses, as shown in Fig. 12. A detailed cost distribution analysis highlights that the expanders represent the largest cost component, accounting for approximately 86.1 % of the annual capital investment. Pumps, compressors, LNG heat exchangers, heat exchangers, and heaters collectively constitute a significantly smaller portion, suggesting that optimizing expander performance and cost could substantially enhance overall economic efficiency. While the inclusion of multiple thermal recovery stages may imply increased capital expenditure, this is effectively mitigated by two key factors: the elimination of mechanical

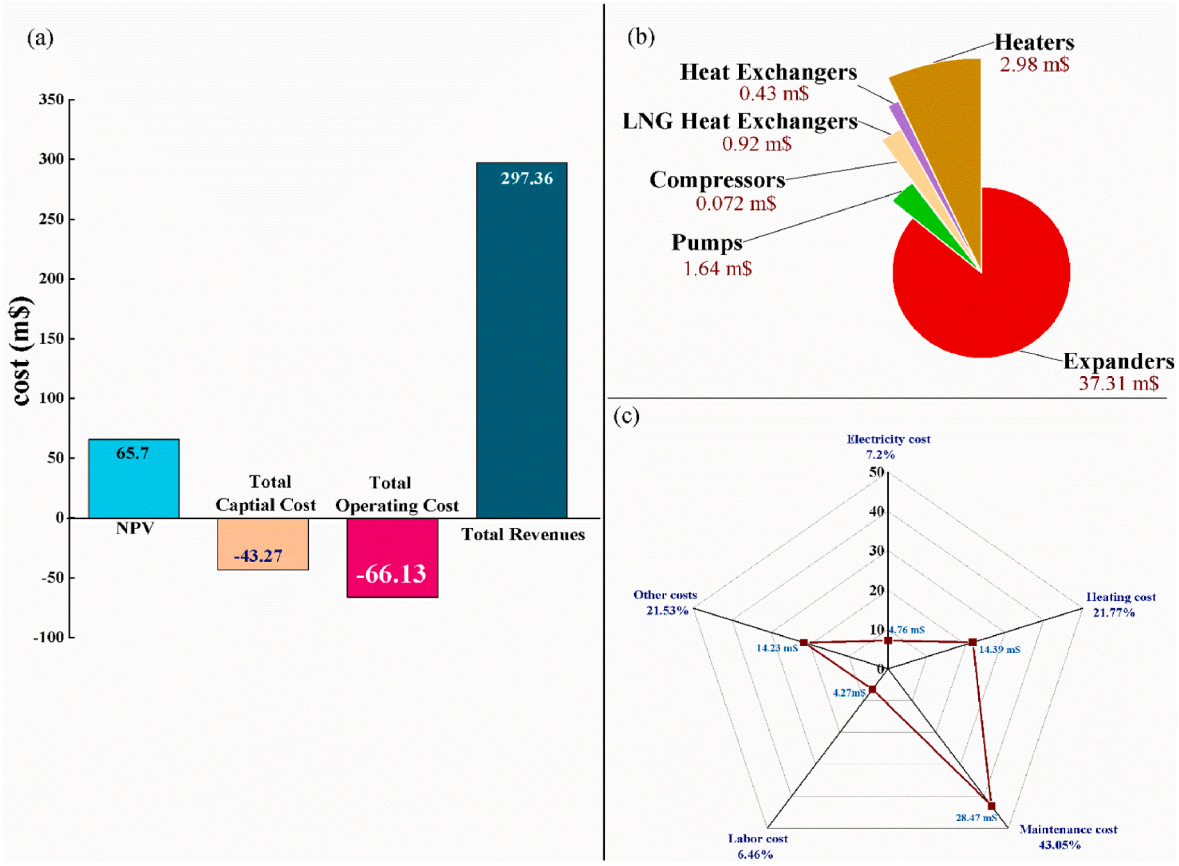

Fig. 11. The proposed system's overall economic analysis results.

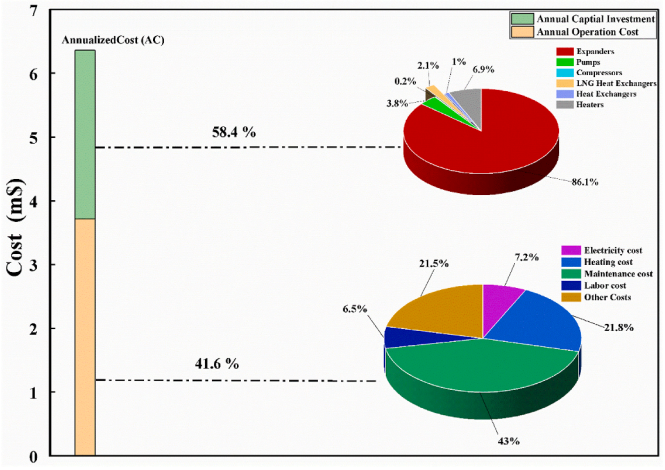

Fig. 12. The annualized cost of the proposed LH_2-N_2R-LAES system.

air compression and the modular architecture of the energy recovery subsystems. The removal of large air compressors—typically one of the most capital-intensive components in conventional LAES systems—reduces fixed infrastructure costs. Furthermore, the modular design allows for configuration flexibility, enabling scale-specific implementation without significant efficiency penalties. As a result, the system maintains favorable economic performance across different capacities.

The Operating costs demonstrate a relatively balanced distribution, with maintenance costs being the most substantial at 43 %, indicating the critical importance of reliability and durability in system design to reduce these recurrent expenses. Heating and other miscellaneous costs closely follow, each representing around 21.8 % and 21.5 %, respectively. Electricity and labor expenses, though lower, at 7.2 % and 6.5 %, respectively, still represent non-negligible costs that could be optimized through improved process integration and automation.

Fig. 13 represents the annual revenue breakdown that highlights significant differences across various operational segments, emphasizing their economic contributions to the integrated LH_2-N_2R-LAES system. The LAES release emerges as the dominant revenue source, generating an annual average revenue of 6.13 million USD, which constitutes 51.5 % of total system revenues. This underlines LAES's critical role within

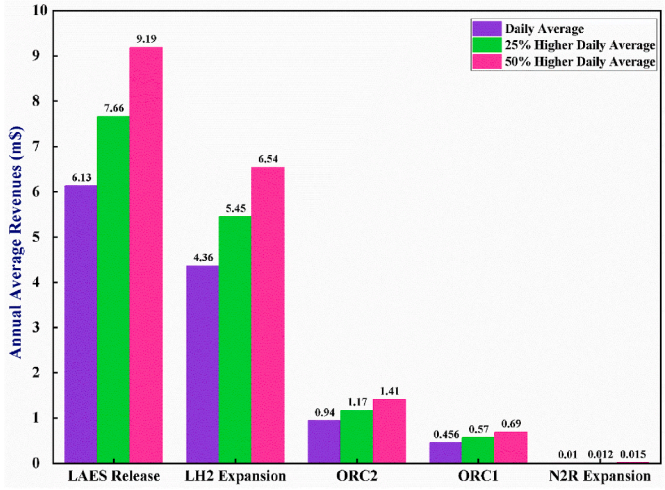

Fig. 13. The annual revenue breakdown across various operational segments.

the overall economic framework, presenting considerable scope for further revenue enhancement, potentially rising to 9.19 million USD under optimistic scenarios of a 50 % increase in daily revenues. Following LAES, LH_2 expansion also substantially contributes, with an annual average revenue of 4.36 million USD, representing approximately 36.7 % of total revenue. Notably, under improved operational conditions (50 % higher daily revenue), LH_2 expansion's revenue potential increases to 6.54 million USD, confirming its significance within the system. In contrast, contributions from the ORC1, ORC2, and N_2R expansion cycles are comparatively modest, accounting for only 3.8 %, 7.9 %, and 0.1 %, respectively, highlighting potential areas for further research and development to optimize these subsystems for enhanced economic benefit. Furthermore, the annualized cost of the system is calculated at 6.36 million USD, with an impressive IRR of 29 % and a PBP of only 2.67 years, reinforcing the strong financial viability of the project, as summarized in Table 4. Overall, the economic analysis underscores the LH_2-N_2R-LAES system's promising profitability potential, driven primarily by efficient capital deployment and significant revenue generation capabilities. In addition to its strong technical and economic performance, the proposed LH_2–N_2R–LAES system offers considerable potential for practical application in the power industry. Its compression-free, fossil-free architecture makes it particularly well-suited for integration with renewable energy sources and hydrogen distribution networks. This can enhance grid flexibility, support peak shaving, and provide firming capacity for variable renewables. The system's high round-trip efficiency and favorable payback period make it economically attractive for large-scale deployment. However, realizing this potential requires addressing several key challenges, including stringent safety requirements for cryogenic hydrogen, the high capital cost of cryogenic components, and the current limitations of global hydrogen infrastructure. Future efforts should focus on pilot-scale demonstration, modular design optimization, and supportive policy frameworks to accelerate commercialization and adoption.

5. Performance benchmarking of the proposed LH_2–N_2R–LAES system

To evaluate the effectiveness and novelty of the proposed LH_2–N_2R–LAES system, a comprehensive benchmarking analysis was conducted against several representative LAES systems reported in recent literature. The comparison, summarized in Table 5, includes key thermodynamic and economic performance indicators such as round-trip efficiency, specific energy consumption, exergy efficiency, net present value, and payback period.

The proposed system exhibits a remarkably high RTE of 329.6 %, significantly outperforming values reported in the literature. For example, Kim et al. reported RTEs of 126.5 % (LH–LAES–WC) and 150.2 % (LH–LAES–WORC), while Zhang et al.'s LNG–ORC–LAES hybrid reached only 45.4 %. Even the advanced LNG–SMR–LAES system proposed by Yehia et al. achieved 168.6 %—still just half of what is attained in the current work. This exceptional RTE is attributed to the synergistic integration of LH_2 regasification and nitrogen expansion (N_2R), which replaces the energy-intensive air compression step with clean, cryogenic cold recovery.

Table 5
Benchmarking of the proposed LH_2–N_2R–LAES system against selected prior LAES Configurations.

System	RTE (%)	SEC (kWh/kg$_{air}$)	Exergy Efficiency (%)	NPV (M$)	PBP (years)
Proposed LH_2-N_2R-LAES system	329.6	0.128	66.0	$65.7	2.67
Kim et al. [18] LH-LAES-WC	126.5	0.117	57.0	32.02	–
Kim et al. [18] LH-LAES-WORC	150.2	0.117	59.7	38.61	–
Zhang et al. [37] LNG–ORC-LAES Hybrid	45.44	0.206	50.73	–	–
Yehia et al. [16] LNG-SMR-LAES	168.6	–	92.03	11.2	1.97

The system also demonstrates excellent liquefaction efficiency, with a specific energy consumption (SEC) of 0.128 kWh/kg-air, lower than Zhang et al.'s 0.206 kWh/kg-air and competitive with the SEC values in Kim et al.'s LH–LAES systems (0.117 kWh/kg-air). The exergy efficiency of 66.0 % further confirms the low irreversibility of the system, surpassing many other configurations, including Kim et al. (57.0–59.7 %) and Zhang et al. (50.73 %), and approaching the optimized LNG–SMR–LAES reported by Yehia et al. (92.03 %).

From an economic perspective, the proposed LH_2–N_2R–LAES system yields a compelling net present value (NPV) of $65.7 million and a payback period (PBP) of 2.67 years, outperforming Yehia et al.'s NPV of $11.2 million and 1.97-year PBP. Other benchmarked systems either lack full techno-economic analysis or demonstrate less favorable investment viability.

In addition to its superior numerical performance, the proposed system distinguishes itself through a fundamentally different architecture. Many reported LAES integrations—particularly those combined with LNG cold recovery—remain dependent on fossil-based energy chains and carry associated carbon burdens. Hybrid LAES–ORC systems typically retain partial mechanical air compression and require complex loop coordination, while sCO_2–LAES designs demand high-pressure turbomachinery and raise concerns regarding working fluid compatibility and operational safety.

By contrast, the LH_2–N_2R–LAES system achieves compression-free direct air liquefaction via integration with two clean and inert cryogenic sources: LH_2 regasification and nitrogen expansion. This design not only simplifies system operation but also ensures enhanced safety, eliminates fossil energy dependency, and aligns with emerging hydrogen-based energy infrastructures. The result is a next-generation LAES configuration that maximizes energy recovery while minimizing system complexity and environmental impact.

6. Conclusion

This study introduces a novel compression-free LAES system that integrates nitrogen expansion refrigeration with Liquefied hydrogen cold energy recovery to achieve sustainable and efficient energy storage. The cold exergy of LH_2 is harnessed to drive both air liquefaction and power generation, eliminating the need for mechanical air compression and significantly reducing parasitic losses. The system features a modular configuration combining N2Rand organic Rankine cycles, enabling enhanced energy integration, system simplicity, and operational flexibility. These design features contribute to improved energy and exergy efficiency while enabling scalable and adaptable deployment across both centralized and distributed energy storage applications. Comprehensive energy, exergy, and economic analyses validate the technical and economic viability of the proposed LH_2–N_2R–LAES system. Key findings include.

- Net energy savings of 3590 kW, contributing to a projected 20.4 % reduction in carbon emissions;
- An exceptional round-trip efficiency of up to 329.62 %, enabled by cryogenic energy recovery.
- A specific energy consumption of 0.13 kWh/kg-air.
- The coefficient of performance of the N_2R cycle was determined to be 1.98.
- A total exergy efficiency of 66 %, reflecting minimized thermodynamic irreversibilities.

- Strong economic indicators, including a Net Present Value of $65.7 million, an Internal Rate of Return of 29 %, and a payback period of 2.67 years.

Compared to conventional LAES systems and other hybrid integrations (e.g., LAES–LNG, LAES–ORC, LAES–sCO_2), this system offers a fossil-free architecture, higher efficiency, and lower system complexity, making it suitable for deployment at hydrogen terminals or energy storage hubs where LH_2 is already available. Its scalability and modularity further support deployment across both centralized and distributed power networks.

The system's multi-stage configuration remains economically viable due to its modular design and the elimination of costly air compression, supporting deployment across various scales. Future research should expand on this foundation by incorporating dynamic operation modeling, investigating part-load behavior and control strategies, and evaluating lifecycle environmental impacts through detailed LCA. Additionally, coupling the model with upstream hydrogen liquefaction or real-time grid response simulations could provide deeper insights into full-chain system integration. The proposed LH_2–N_2R–LAES system thus represents a promising direction for high-efficiency, compression-free, and fossil-independent energy storage aligned with global decarbonization goals.

CRediT authorship contribution statement

Fatma Yehia: Writing – review & editing, Writing – original draft, Visualization, Validation, Software, Resources, Project administration, Methodology, Investigation, Funding acquisition, Formal analysis, Data curation, Conceptualization. **Akram Ali Nasser Mansoor Al-Haimi:** Writing – review & editing, Writing – original draft, Visualization, Validation, Software, Resources, Project administration, Methodology, Investigation, Funding acquisition, Formal analysis, Data curation, Conceptualization. **Yuree Byun:** Software, Resources, Methodology, Investigation, Formal analysis. **Junseok Kim:** Methodology, Investigation, Formal analysis, Data curation, Conceptualization. **Chuangji Feng:** Software, Investigation, Formal analysis. **Yu Cao:** Software, Resources, Methodology, Investigation, Data curation. **Yesom Yun:** Visualization, Software, Resources, Methodology, Investigation, Formal analysis, Data curation, Conceptualization. **Jeongwon Kim:** Methodology, Investigation, Formal analysis, Conceptualization. **Chao Yang:** Writing – review & editing, Supervision, Project administration, Funding acquisition. **Lihua Liu:** Writing – review & editing, Supervision, Project administration, Investigation, Funding acquisition. **Jihyun Hwang:** Writing – review & editing, Visualization, Validation, Supervision, Software, Resources, Project administration, Methodology, Investigation, Funding acquisition, Formal analysis, Data curation, Conceptualization.

Declaration of competing interest

The authors state that they do not have any competing financial interests or personal relationships that could have influenced the work reported in this paper.

Acknowledgments

This research was supported by Korea Institute of Marine Science & Technology Promotion (KIMST) funded by the Ministry of Oceans and Fisheries (2520000248). The authors gratefully acknowledge the financial support provided by the Alliance of International Science Organizations (ANSO) through the ANSO Scholarship for Young Talents at the University of Science and Technology of China (USTC).

Appendix A. Supplementary data

Supplementary data to this article can be found online at https://doi.org/10.1016/j.energy.2025.137542.

Nomenclature

Abbreviations			
LAES	Liquid air energy storage	H	Seawater heater
LH_2	Liquefied hydrogen	T-S	Temperature-entropy
N_2R	Nitrogen refrigeration	K	Compressor
LNG	Liquefied natural gas	P-H	Pressure-enthalpy
RTE	Round-trip efficiency	T	Expander
RRCs	Regenerative Rankine cycles	para-H_2	Para-hydrogen
ORC	Organic rankine cycle	MTD	Minimum temperature difference
LCOE	Levelized cost of energy	SEC	Specific energy consumption
GH_2	Hydrogen gas	COP	Coefficient of N_2R performance
P	Pump	NPV	Net present value
LA	Liquid Air	THCC	Temperature and heat composite curves
HXs	Heat exchanger	TDCC	Temperature difference composite curves
BM	Bare module	IRR	Internal rate of return
CRF	Capital recovery factor	PBP	Payback period
LMTD	Log mean temperature difference		
Symbols & Subscripts			
$\mathbf{P_{net,out}}$	Total power outputs	S	Entropy in the system's streams
$\mathbf{P_{net,in}}$	Total power inputs	EXE_{net_in}	Net exergy input
$\boldsymbol{\varpi_{En,R}}$	Energy released	EXE_{in}	Total exergy Input
$\boldsymbol{\varpi_{En,S}}$	Energy stored	W_{in}	Input work
$\mathbf{W_{ORC1}}$	Power generated by first ORC		
$\mathbf{W_{ORC2}}$	Power generated by second ORC	EXE_{net_out}	Net exergy output
$\mathbf{W_{N2R}}$	Power generated by N_2R Cycle	EXE_{out}	Total exergy output
$\mathbf{W_{T,i}}$	Power generated by expansion systems	W_{out}	Work generated
$\mathbf{W_{p,i}}$	Power consumed by pumps	$EXE_{net-destruction}$	Total exergy destruction
$\mathbf{W_{k,N2R}}$	Power consumed by compressors	C_{TCI}	Total capital investment
$\mathbf{Q_{LH2}}$	Cold energy supplied by liquid hydrogen	ω	Operating years
$\mathbf{Q_{N2R}}$	Cold energy supplied by nitrogen expansion cycle	n	Plant's life

(*continued on next page*)

(*continued*)

Abbreviations			
$\mathbf{T_{on-peak}}$	Power-release time	τ	Discount rate
$\mathbf{m_{N_2}}$	Mass flow rate of the N_2R working fluid	S_T	Annual sales revenue
$\mathbf{h_{N_2\ in}}$	Enthalpy of the inlet stream	C_{oc}	Annual operating costs
$\mathbf{h_{N_2\ out}}$	N_2 Enthalpy outlet stream	C_{Dep}	Depreciation costs
$\mathbf{W_{total}}$	Total work input	φ	Tax rate
EXE	Exergy rate	$C_{BM,i}$	Cost approach
h	Enthalpy	$C^0_{p,i}$	Purchased cost function
T	Temperature		

Data availability

Data will be made available on request.

References

[1] Yang X, Bulushev DA, Yang J, Zhang Q. New liquid chemical hydrogen storage technology. Energies 2022;15(17):6360.
[2] Rabi AM, Radulovic J, Buick JM. Comprehensive review of Liquid Air Energy Storage (LAES) technologies. Energies 2023;16(17):6216.
[3] Shi X, He Q, Liu Y, Zhang Q, An X, Du D. Design and analysis of a novel liquefied air energy storage system coupled with coal-fired power unit. J Energy Storage 2023;73:109204.
[4] Morgan R, Nelmes S, Gibson E, Brett G. Liquid air energy storage–analysis and first results from a pilot scale demonstration plant. Appl Energy 2015;137:845–53.
[5] Adedeji M, Abid M, Dagbasi M, Adun H, Adebayo V. Improvement of a liquid air energy storage system: investigation of performance analysis for novel ambient air conditioning. J Energy Storage 2022;50:104294.
[6] Xue X, Wang S, Zhang X, Cui C, Chen L, Zhou Y, Wang J. Thermodynamic analysis of a novel liquid air energy storage system. Phys Procedia 2015;67:733–8.
[7] Guizzi GL, Manno M, Tolomei LM, Vitali RM. Thermodynamic analysis of a liquid air energy storage system. Energy 2015;93:1639–47.
[8] Guo L, Ji W, Gao Z, Fan X, Wang J. Dynamic characteristics analysis of the cold energy transfer in the liquid air energy storage system based on different modes of packed bed. J Energy Storage 2021;40:102712.
[9] Wang C, Cui Q, Dai Z, Zhang X, Xue L, You Z, She X. Performance analysis of liquid air energy storage with enhanced cold storage density for combined heating and power generation. J Energy Storage 2022;46:103836.
[10] Zhang Z, Ding T, Zhou Q, Sun Y, Qu M, Zeng Z, et al. A review of technologies and applications on versatile energy storage systems. Renew Sustain Energy Rev 2021;148:111263.
[11] O'Callaghan O, Donnellan P. Liquid air energy storage systems: a review. Renew Sustain Energy Rev 2021;146:111113.
[12] Fan M, Liu C, Tong L, Yin S, Zuo Z, Wang L, Ding Y. A cold thermal energy storage based on ASU-LAES system: energy, exergy, and economic analysis. Energy 2025;314:134132.
[13] Salem AM, Khaira AM. A mini-review on liquid air energy storage system hybridization, modelling, and economics: towards carbon neutrality. RSC Adv 2023;13(38):26380–91.
[14] Naquash A, Riaz A, Qyyum MA, Aziz M, Assareh E, Lee M. Liquid hydrogen storage and regasification process integrated with LNG, NGL, and liquid helium production. Renew Energy 2023;213:165–75.
[15] Park J, You F, Cho H, Lee I, Moon I. Novel massive thermal energy storage system for liquefied natural gas cold energy recovery. Energy 2020;195:117022.
[16] Yehia F, Al-Haimi AANM, Byun Y, Kim J, Yun Y, Lee G, et al. Integration of the single-effect mixed refrigerant cycle with liquified air energy storage and cold energy of LNG regasification: energy, exergy, and efficiency prospectives. Energy 2024;306:132567.
[17] Park J, Cho S, Qi M, Noh W, Lee I, Moon I. Liquid air energy storage coupled with liquefied natural gas cold energy: focus on efficiency, energy capacity, and flexibility. Energy 2021;216:119308.
[18] Kim Y, Qi M, Cho J, Lee I, Park J, Moon I. Process design and analysis for combined hydrogen regasification process and liquid air energy storage. Energy 2023;283:129093.
[19] Ansarinasab H, Fatimah M, Khojasteh-Salkuyeh Y. Performance improvement of air liquefaction processes for liquid air energy storage (LAES) using magnetic refrigeration system. J Energy Storage 2023;65:107304.
[20] Trevisani L, Fabbri M, Negrini F, Ribani P. Advanced energy recovery systems from liquid hydrogen. Energy Convers Manag 2007;48(1):146–54.
[21] Gahleitner G. Hydrogen from renewable electricity: an international review of power-to-gas pilot plants for stationary applications. Int J Hydrogen Energy 2013;38(5):2039–61.
[22] Cardella U, Decker L, Klein H. Economically viable large-scale hydrogen liquefaction. Conference economically viable large-scale hydrogen liquefaction, vol. vol 171. IOP Publishing, p. 012013.
[23] Kim A, Yoo Y, Kim S, Lim H. Comprehensive analysis of overall H2 supply for different H2 carriers from overseas production to inland distribution with respect to economic, environmental, and technological aspects. Renew Energy 2021;177:422–32.
[24] Taylor J, Alderson J, Kalyanam K, Lyle A, Phillips L. Technical and economic assessment of methods for the storage of large quantities of hydrogen. Int J Hydrogen Energy 1986;11(1):5–22.
[25] Steward D, Saur G, Penev M, Ramsden T. In: Medium, editor. Lifecycle cost analysis of hydrogen versus other technologies for electrical energy storage. United States: National Renewable Energy Lab. (NREL), Golden, CO (United States); 2009. Size: 59.
[26] Voth R, Parrish W. Studies of hydrogen liquefier efficiency and the recovery of the liquefaction energy. 1977.
[27] Laouir A. Performance analysis of open-loop cycles for LH2 regasification. Int J Hydrogen Energy 2019;44(39):22425–36.
[28] Furuhama S, Nakajima T, Honda T. Rankine cycle engines for utilization of LH2 car fuel as a low-temperature source. Int J Hydrogen Energy 1993;18(2):149–55.
[29] Incer-Valverde J, Lugo-Mayor C, Tsatsaronis G, Morosuk T. Evaluation of the large-scale hydrogen supply chain and perspectives on LH2 regasification cogeneration systems. Gas Sci Eng 2023;115:205005.
[30] Mun H, Kim Y, Park J, Lee I. Power generation system utilizing cold energy from liquid hydrogen: integration with a liquid air storage system for peak load shaving. Energy 2024;306:132351.
[31] Zhang N, Lior N. A novel Brayton cycle with the integration of liquid hydrogen cryogenic exergy utilization. Int J Hydrogen Energy 2008;33(1):214–24.
[32] Yu Y, Xie F, Li Y. Study on recovery and utilization of cold energy for insulation design of liquid hydrogen tanks. Energy 2024;310:133167.
[33] Kim Y, Mun H, Kim M, Moon I, Park J, Lee I, Kim J. Design and global sensitivity analysis of a flexible hydrogen regasification process integrated with liquid air energy storage system. Energy 2025;316:134533.
[34] Braimakis K, Karellas S. Chapter 12 - organic Rankine cycle systems for waste heat recovery in thermal power plants. In: Desideri U, Ferrari L, editors. Small scale power generation. Handbook: Academic Press; 2025. p. 309–39.
[35] Quoilin S, Broek MVD, Declaye S, Dewallef P, Lemort V. Techno-economic survey of Organic Rankine Cycle (ORC) systems. Renew Sustain Energy Rev 2013;22:168–86.
[36] She X, Peng X, Nie B, Leng G, Zhang X, Weng L, et al. Enhancement of round trip efficiency of liquid air energy storage through effective utilization of heat of compression. Appl Energy 2017;206:1632–42.
[37] Zhang T, Chen L, Zhang X, Mei S, Xue X, Zhou Y. Thermodynamic analysis of a novel hybrid liquid air energy storage system based on the utilization of LNG cold energy. Energy 2018;155:641–50.
[38] Peng X, She X, Li C, Luo Y, Zhang T, Li Y, Ding Y. Liquid air energy storage flexibly coupled with LNG regasification for improving air liquefaction. Appl Energy 2019;250:1190–201.
[39] Kim HS. 4E analysis of novel direct expansion cycle-organic Rankine cycle-integrated hydrogen refueling station system using liquid hydrogen cold energy. J Clean Prod 2024;462:142682.
[40] Wang L, He L, He Y. Review on absorption refrigeration technology and its potential in energy-saving and carbon emission reduction in natural gas and hydrogen liquefaction. Energies 2024;17(14):3427.
[41] Ross Jr RG. Refrigeration systems for achieving cryogenic temperatures. Low temperature materials and mechanisms. CRC Press; 2016. p. 127–200.
[42] Popov D, Fikiin K, Stankov B, Alvarez G, Youbi-Idrissi M, Damas A, et al. Cryogenic heat exchangers for process cooling and renewable energy storage: a review. Appl Therm Eng 2019;153:275–90.
[43] Laut PB, Johnstone DW. Use nitrogen to boost plant safety and product quality. Chem Eng 1994;101(6):96.
[44] Biglia A, Bilardo M, Comba L, Aimonino DR, Grella M, Fabrizio E, Gay P. Performance analysis of a nitrogen-based Brayton cryocooler prototype. Energy 2024;290:130095.
[45] Vecchi A, Li Y, Ding Y, Mancarella P, Sciacovelli A. Liquid air energy storage (LAES): a review on technology state-of-the-art, integration pathways and future perspectives. Adv Appl Energy 2021;3:100047.
[46] Riaz A, Qyyum MA, Hussain A, Lee M. Tapping the energy and exergy benefits of channeling liquid air energy system in the hydrogen liquefaction process. J Energy Storage 2023;72:108193.
[47] Chenchen W, Zhang J, Yu X, Tang Q. Integration of nitrogen refrigeration in an lng-coupled liquid air energy storage System: performance optimization and economic analysis. Available at SSRN 5056395.

[48] Zhang J, Chenchen W, Yu X, Tang Q. Thermodynamic analysis of a laes system coupled with Lng Cold energy and nitrogen expansion refrigeration. Available at SSRN 5015618 2024.
[49] Afonso J, Catarino I, Patrício R, Rocaboy A, Linder M, Bonfait G. Liquid nitrogen energy storage unit. Cryogenics 2011;51(11–12):621–9.
[50] Bao J, Zhao L. A review of working fluid and expander selections for organic Rankine cycle. Renew Sustain Energy Rev 2013;24:325–42.
[51] Chen H, Goswami DY, Stefanakos EK. A review of thermodynamic cycles and working fluids for the conversion of low-grade heat. Renew Sustain Energy Rev 2010;14(9):3059–67.
[52] Lecompte S, Huisseune H, van den Broek M, De Paepe M. Methodical thermodynamic analysis and regression models of organic Rankine cycle architectures for waste heat recovery. Energy 2015;87:60–76.
[53] Penev M, Zuboy J, Hunter C. Economic analysis of a high-pressure urban pipeline concept (HyLine) for delivering hydrogen to retail fueling stations. Transport Res Transport Environ 2019;77:92–105.
[54] Gil Chaves ID, López JRG, García Zapata JL, Leguizamón Robayo A, Rodríguez Niño G, Chaves IDG, et al. Thermodynamic and property models. Process Analysis and Simulation in Chemical Engineering 2016:53–102.
[55] Lopez-Echeverry JS, Reif-Acherman S, Araujo-Lopez E. Peng-Robinson equation of state: 40 years through cubics. Fluid Phase Equilib 2017;447:39–71.
[56] Jacobsen RT, Penoncello SG, Lemmon EW, Jacobsen RT, Penoncello SG, Lemmon EW. Thermodynamic properties of cryogenic fluids. Springer; 1997.
[57] Naquash A, Qyyum MA, Islam M, Sial NR, Min S, Lee S, Lee M. Performance enhancement of hydrogen liquefaction process via absorption refrigeration and organic Rankine cycle-assisted liquid air energy system. Energy Convers Manag 2022;254:115200.
[58] Aasadnia M, Mehrpooya M. Large-scale liquid hydrogen production methods and approaches: a review. Appl Energy 2018;212:57–83.
[59] Kwon H, Park J, Koo B. 4E analysis for a novel cryogenic hydrogen liquefaction process using various refrigerants: energy, exergy, economic, and environment. J Clean Prod 2024;469:143146.
[60] Lozano-Martín D, Moreau A, Chamorro CR. Thermophysical properties of hydrogen mixtures relevant for the development of the hydrogen economy: review of available experimental data and thermodynamic models. Renew Energy 2022;198:1398–429.
[61] Lee I, Park J, Moon I. Conceptual design and exergy analysis of combined cryogenic energy storage and LNG regasification processes: cold and power integration. Energy 2017;140:106–15.
[62] Qi M, Park J, Kim J, Lee I, Moon I. Advanced integration of LNG regasification power plant with liquid air energy storage: enhancements in flexibility, safety, and power generation. Appl Energy 2020;269:115049.
[63] Ameel B, T'Joen C, De Kerpel K, De Jaeger P, Huisseune H, Van Belleghem M, De Paepe M. Thermodynamic analysis of energy storage with a liquid air Rankine cycle. Appl Therm Eng 2013;52(1):130–40.
[64] Damak C, Leducq D, Hoang HM, Negro D, Delahaye A. Liquid Air Energy Storage (LAES) as a large-scale storage technology for renewable energy integration–A review of investigation studies and near perspectives of LAES. Int J Refrig 2020;110:208–18.
[65] Li Y, Cao H, Wang S, Jin Y, Li D, Wang X, Ding Y. Load shifting of nuclear power plants using cryogenic energy storage technology. Appl Energy 2014;113:1710–6.
[66] Ding X, Duan L, Zhou Y, Gao C, Bao Y. Energy, exergy, and economic analyses of a new liquid air energy storage system coupled with solar heat and organic Rankine cycle. Energy Convers Manag 2022;266:115828.
[67] Terzi R. Application of exergy analysis to energy systems. Application of exergy, vol 109; 2018.
[68] Peters MS, Timmerhaus KD, West RE. Plant design and economics for chemical engineers. New York: McGraw-hill; 2003.
[69] Turton R, Bailie RC, Whiting WB, Shaeiwitz JA. Analysis, synthesis and design of chemical processes. Pearson Education; 2008.
[70] Naquash A, Qyyum MA, Chaniago YD, Riaz A, Yehia F, Lim H, Lee M. Separation and purification of syngas-derived hydrogen: a comparative evaluation of membrane- and cryogenic-assisted approaches. Chemosphere 2023;313:137420.
[71] Davison J. Criteria for technical and economic assessment of plants with low CO2 emissions. Cheltenham, UK: IEA Greenhouse Gas R & D Programme; 2009.
[72] Overview of business valuation parameters in the energy industry. edition n.3. Deloitte; 2017.
[73] Asen E. Corporate tax rates around the world, 2020. The Tax Foundation; 2020.
[74] Global electricity prices in 2018. https://www.statista.com/statistics/263492/electricity-prices-in-selected-countries/.
[75] Park J, Lee I, You F, Moon I. Economic process selection of liquefied natural gas regasification: power generation and energy storage applications. Ind Eng Chem Res 2019;58(12):4946–56.
[76] Lee I, Moon I. Economic optimization of dual mixed refrigerant liquefied natural gas plant considering natural gas extraction rate. Ind Eng Chem Res 2017;56(10):2804–14.
[77] Lee I, Moon I. Total cost optimization of a single mixed refrigerant process based on equipment cost and life expectancy. Ind Eng Chem Res 2016;55(39):10336–43.
[78] Wang G-B, Zhang X-R. Thermodynamic analysis of a novel pumped thermal energy storage system utilizing ambient thermal energy and LNG cold energy. Energy Convers Manag 2017;148:1248–64.
[79] Bi Y, Ju Y. Design and analysis of an efficient hydrogen liquefaction process based on helium reverse Brayton cycle integrating with steam methane reforming and liquefied natural gas cold energy utilization. Energy 2022;252:124047.